Journal of Engineering and Applied Sciences 13 (Special Issue 9): 7081-7085, 2018
ISSN: 1816-949X


# Morphological Interpolations of Low-Resolution DEMs vs. High-Resolution DEMS: A Comparative Study

[1]Sin Liang Lim, [2]Sim-Hui Tee and [3]Sin Ting Lim
[1]Faculty of Engineering,
[2]Faculty of Creative Multimedia,
[3]Faculty of Engineering and Technology, Multimedia University, Persiaran Multimedia,
63100 Cyberjaya, Selangor, Malaysia

**Abstract:** This study analyzes the morphological medians generated hierarchically between two sets of Digital Elevation Models (DEMs): a pair of low-resolution DEM acquired from an online resource which is freely available to researchers and academician and another pair of higher-resolution DEMs obtained from an agency. Using morphological approach, the interpolated sequences between these two pairs of DEMs at low-and high-resolution are generated. These hierarchically sequential morphing-like medians provides a way to visualize the spatiotemporal changes that have occurred between the source and target DEMs at discrete-time intervals and episodic intervals.

**Key words:** Digital Elevation Modem (DEM), dilation, erosion, mathematical morphology, morphological, Malaysia

## INTRODUCTION

Spatial maps are multivalued functions which represent various phenomena across spatial positions. Examples of spatial maps include digital elevation maps, grayscale images, bathymetric maps, rainfall values or any spatial fields related to ecology, geomorphology, environmental, geohazard, archaeology, etc. With the advancement of technology, acquisition of such spatial maps at multiple spatial and temporal scales are available through remote sensing, surveys and historical records. However, to acquire data at continuous manner is very costly in terms of manpower, time and other resources. As a result, in this study, we propose using a morphological approach to visualize the interpolated episode between a pair of spatial maps one at lower resolution and the other at higher resolution to observe the changes in between. The spatial maps of interest are Digital Elevation Model (DEM)s. By generating the morphological medians hierarchically in between a pair of DEMs via. nonlinear morphological operations, a morphing-like sequence will be produced to assist visualization of changes that occur over time.

DEM is a rasterized 3-dimentional representation of the surface of a terrain and it is usually modeled using remote sensing system (Shingare and Kale, 2013). A point in DEM data represents the elevation value for each cell in a specific cell size. DEM data is very important in many aspects of studies. Applications of DEM data can be found in Geographic Information System (GIS), water flow modelling, landslide monitoring, flight simulation and many more. There are many work done which demonstrates the numerous areas which DEM can be applied. These include using DEM to represent the land surface to simulate the hydrologic process (Zhang and Montgomery, 1994), modelling the flow over hill slopes (Costa-Cabral and Burges, 1994) and predicting watershed model in the aspect of hydrology by using different DEM resolution or DEM map scale (Wolock and Price, 1994).

Numerous interpolation techniques such as Kriging, Inverse Distance Weighting (IDW) and Spline are commonly adopted in generating DEM at different scales (Arun, 2013; Erdogan, 2009). However, in this study, we will not discuss about the interpolation methods to construct DEMs at the field scale but we focus on visualizing the continuous sequence from a source-DEM to a target-DEM. This morphing-like sequence at temporal intervals between the pairs of DEMs data could help us to study the temporal changes which evolve from source-DEM to target-DEM. The proposed methods by Serra (1983, 1998), Beucher (1994), Soille (1994), Meyer (1994, 1996), Iwanowski and Serra (2000) and Iwanowski (2000, 2002) dealt with the generation of interpolated

**Corresponding Author:** Sin Liang Lim, Faculty of Engineering, Multimedia University, Persiaran Multimedia, 63100 Cyberjaya, Selangor, Malaysia

sequences in binary (black/white) form spatial objects. In our study, the DEMs are represented in grayscale instead of binary.

Mathematical morphology concept is based on set theory (Serra, 1983) and it has been proven robust and successful in processing and analyzing digital images, including spatial interpolations (Serra, 1998; Beucher, 1994; Iwanowski and Serra, 2000; Iwanowski, 2000). In this study, we adopt the framework as proposed in on two pairs of DEMs which are of significantly different resolutions. The higher resolution data are acquired from Malaysian Centre for Geospatial Data Infrastructure (MaCGDI) while the lower resolution data (ASTER Global Digital Elevation Model (ASTER GDEM)) is downloaded online from Japan Space Systems (JSS) website which is freely available to researchers and academician. It will be interesting to visualize the interpolated sequences generated from two sets of DEM pairs. If the interpolation results between the DEM pairs are similar then we can suggest that the interpolated sequence acquired from the ASTER GDEM data by JSS as an alternative resource, as compared to the privately owned higher resolution DEM data. Higher resolution DEM data is usually privately owned and thus restricted, some of which incur cost.

## MATERIALS AND METHODS

**Mathematical morphology:** Digital image is an array containing discrete values at each (x, y) position. Let f(x, y) represents a grayscale image which assumes Z+1 possible intensity values where m = 0, 1, 2, …, M. Since, the image is denoted as gray level, thus, each pixel is assigned with 8 bit which leads to M = 255.

**Grayscale morphological operations:** Grayscale morphological dilation and erosion transformations of f(x, y) (Fig. 1a) with respect to a flat structuring element B (Fig. 1b) are defined, respectively as:

$$(f \oplus B)(x, y) = \max_{(i, j)\in B} \{(x\text{-}i, y\text{-}j)\} \quad (1)$$

$$(f \Theta B)(x, y) = \min_{(i, j)\in B} \{(x+i, y+j)\} \quad (2)$$

where, ⊕ and Θ are symbols used to denote dilation and erosion, respectively. The structuring element B considered is flat, symmetric about origin, rhombic in shape and has a primitive size of 3×3 as shown in Fig. 1b. The dilation and erosion of image f (x, y) with respect

(a)

| | | | | |
|---|---|---|---|---|
| 92 | 183 | 250 | 200 | 191 |
| 160 | 145 | 89 | 68 | 54 |
| 32 | 70 | 120 | 53 | 136 |
| 9 | 101 | 44 | 60 | 98 |
| 122 | 83 | 72 | 125 | 5 |

(b)

| | | |
|---|---|---|
| 0 | 1 | 0 |
| 1 | 1 | 1 |
| 0 | 1 | 0 |

(c)

| | | | | |
|---|---|---|---|---|
| 183 | 250 | 250 | 250 | 200 |
| 160 | 183 | 250 | 200 | 191 |
| 160 | 145 | 120 | 136 | 136 |
| 122 | 101 | 120 | 125 | 136 |
| 122 | 122 | 125 | 125 | 125 |

(d)

| | | | | |
|---|---|---|---|---|
| 92 | 92 | 89 | 68 | 54 |
| 32 | 70 | 68 | 53 | 54 |
| 9 | 32 | 44 | 53 | 53 |
| 9 | 9 | 44 | 44 | 5 |
| 9 | 72 | 44 | 5 | 5 |

(e)

| | | | | |
|---|---|---|---|---|
| 92 | 92 | 92 | 89 | 68 |
| 92 | 92 | 89 | 68 | 54 |
| 32 | 70 | 68 | 53 | 54 |
| 9 | 72 | 44 | 53 | 53 |
| 72 | 72 | 72 | 44 | 5 |

(f)

| | | | | |
|---|---|---|---|---|
| 160 | 183 | 250 | 200 | 191 |
| 160 | 145 | 120 | 136 | 136 |
| 122 | 101 | 120 | 120 | 136 |
| 101 | 101 | 101 | 120 | 125 |
| 122 | 101 | 120 | 125 | 125 |

Fig. 1: a) Grayscale image, f(x, y); b) Structuring element B of primitive size 3×3; c) Dilation; d) Erosion; e) Opening and f) Closing of f(x, y) with respect to B

to structuring element B are shown in Fig. 1c and d. Dilation transformation fills the central values in the neighborhood image with the maximum gray values while erosion takes the central values as the minimum gray values within the neighborhood image. As a result, dilation brightens the original image while erosion darkens the image. The combination of dilation and erosion leads to two other morphological operations, i.e., opening and closing. Opening of f by B is achieved by eroding f then the resultant image is dilated. In contrast, closing is obtained by performing dilation of f first, then followed by eroding the resultant image. In this way, opening is the dual of closing. Mathematically, opening and closing is represented in Eq. 3 and 4 as:

$$(f \circ B)(x, y) = (f \Theta B) \oplus B \quad (3)$$

$$(f \bullet B)(x, y) = (f \oplus B) \Theta B \quad (4)$$

where $\circ$ and $\bullet$ are symbols used to denote opening and closing, respectively. Opening Fig. 1e tends to remove particular image details which are smaller than B while closing fills holes in objects and connects small breaks.

**Multiscale grayscale morphological operations:** Multiscale operations can be constructed by increasing the size of nB where n = 0, 1, 2, 3, ..., N. For instance to generate multiscale erosion ($f\Theta nB$) is equivalent to generating iterative dilation by primitive size of B by n times as shown in Eq. 5:

$$(f \Theta nB) = (f \Theta B) \Theta B \Theta B, ..., \Theta B \quad (5)$$

Multiscale dilation, opening and closings can also be generated by following similar manner as expressed below:

$$(f \oplus nB) = (f \oplus B) \oplus B \oplus B, ..., \oplus B \quad (6)$$

$$(f \circ nB) = (f \circ B) \circ B \circ B, ..., \circ B \quad (7)$$

$$(f \bullet nB) = (f \bullet B) \bullet B \bullet B, ..., \bullet B \quad (8)$$

at scale n = 0, 1, 2, 3, …, N. Furthermore, in order to determine the number of iterations required to hierarchically compute 15 (up to 4 levels or $2^4$-1) used in section 5, we need to compute the area of f, denoted as A(f) as the summation of all data values spread across the (x, y) positions in the image or simply $A(f) = \sum_{x,y} f(x, y)$.

**Infima and suprema of f and g:** Assuming that f and g represent two DEMs in grayscale and let infima ($f \wedge g$) and suprema ($f \vee g$) of these DEMs be denoted as:

$$(f \wedge g) = \inf(f, g) = \min\{f(x,y), g(x, y)\} \quad (9)$$

$$(f \vee g) = \sup(f, g) = \max\{f(x, y), g(x, y)\} \quad (10)$$

**Morphological median:** According to the morphological median between f and g, given as M(f, g) can be obtained as:

$$M(f, g) = \bigvee_{n=0}^{N} (M_n(f, g)) \quad (11)$$

where:

$$M_n(f, g) = ((f \wedge g) \oplus nB) \wedge ((f \vee g) \Theta nB) \quad (12)$$

**Dem data and study area:** The study area encompasses the tea plantation, vegetable farm, forest and grassland in Cameron highlands, Malaysia. Cameron highlands is a mountainous area with elevation up to 1600 m above sea level. Under ideal case it is best if we could obtain the sets of DEM data of the same areas over different time to study the changes which happen over the periods. However, since, we only have a set of DEM data, we decide to select two different areas in the same period in order to observe the morphological changes. Nonetheless, the areas covered by MaCGDI DEM and ASTER GDEM are the same,as shown in Fig. 2. Although, Fig. 2a, b as well as Fig. 2c and d look similar, they are

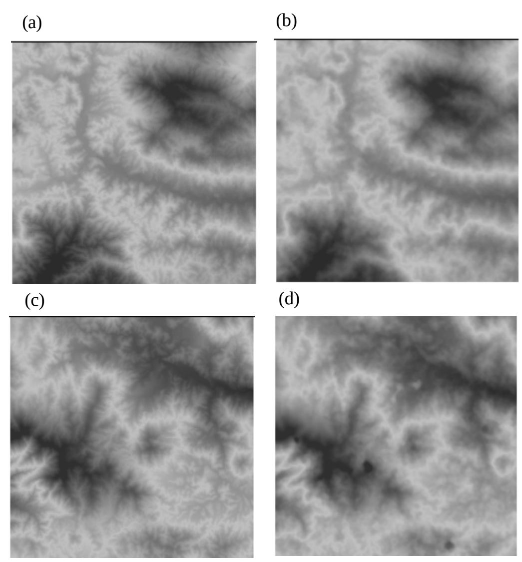


Fig. 2: Study region: a) Original Area 1 from MaCGDI DEM; b) Area 1 from ASTER GDEM; c) Original Area 2 from MaCGDI DEM and d) Area 2 from ASTER GDEM

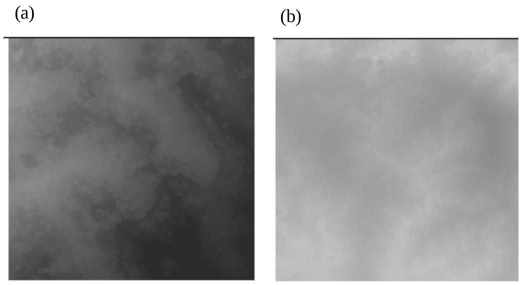


Fig. 3: A subset of study region for MaCGDI DEM: a) Area 1 and b) Area 2

actually of significantly different resolutions. For area 1, the original resolution for MaCGDI DEM is 9841×9841 pixels. However, due to computation limitation in MATLAB Software, we have no choice but to pick a smaller area in area 1 and 2 for MacGDI DEM such that the resolution is reduced to 1024×1024 pixels as shown in Fig. 3. For ASTER GDEM data, the resolution of area 1 and 2 is 257×258 pixels. For area 1, the latitude covers 4°22' 7 "N-4°27'14 "N and longitude of 101°22' 4"E-101°26'18"E. As for area 2, the latitude ranges from 4°29'32"N-4°33'49"N and longitude of 101°22'2.842"E-101°26'17.485"E. In each figure, higher grayscale values in DEMs denote higher elevation values and vice versa. We adopted the approach as explained in section 2 in order to hierarchically construct the morphological medians between these two pairs of DEMs.

## RESULTS AND DISCUSSION

Starting from zeroth level to the third level, successive levels of morphological medians are generated by using flat structuring element Fig. 1b at primitive size of 3×3 pixels. In total, 15 morphological medians are generated between area 1 and 2 including one zeroth-level, two first-level, four second-level and eight third-level morphological medians. The sequential morphological medians resulted from these pairs of MaCGDI DEM and ASTER GDEM are shown in Fig. 4 and 5, respectively.

The simulation is run on a machine with Windows 10 as operating system, Intel Core i5 processor and 4 GB of RAM. However, it is regretted that due to restrictions in MATLAB Software, we are unable to make a fair comparison of interpolation results between area 1 and 2 from the higher-resolution MaCGDI DEM and lower-resolution ASTER GDEM. However, we hope that the work-around method of using smaller area of MacGDI DEM could give us a close comparison. Based on the results shown in Fig. 5, we are quite certain that the morphological interpolations generated from ASTER GDEM give rather smooth transition from one DEM to another DEM. Furthermore, it is obvious from Fig. 6 that ASTER GDEM takes significantly lesser number of iterations to reach the convergence level. In other words, ASTER GDEM converge faster than MaCGDI DEM even though smaller area of MaCGDI DEM is adopted. In addition in terms of elapsed time, ASTER GDEM takes about 25 min processing time while MaCGDI DEM takes about 5 h to complete the computation, despite smaller study region is used for MaCGDI DEM.

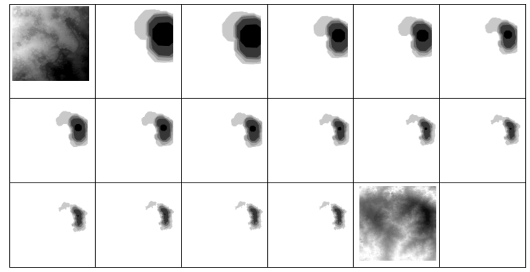

Fig. 4: Grayscale morphological medians generated for smaller regions of MaCGDI DEM

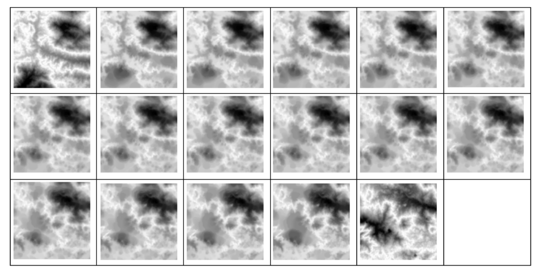

Fig. 5: Grayscale morphological medians generated for ASTER GDEM

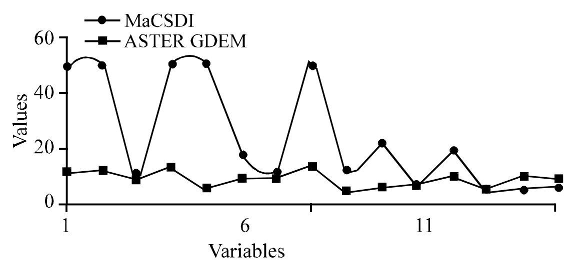


Fig. 6: Number of iterations required to hierarchically generate 15 (up to 4 levels or $2^4$-1) morphological medians between area 1 and 2 of MaCGDI DEM and ASTER GDEM, respectively

## CONCLUSION

In this study, we investigate the possibility of generating grayscale morphological interpolations between two types of DEM data: higher-resolution

MaCGDI DEM vs. lower-resolution ASTER GDEM. These hierarchically computed morphological medians metamorphose from a source-DEM into a target-DEM (area 1 and 2). Based on the results obtained it is found that the morphing generated from ASTER GDEM produces smoother transition from source-DEM to target-DEM across discrete time steps as compared to MaCGDI DEM. Besides it also, requires less computation time and less number of iterations to achieve the convergence level. As such it is concluded that, the freely available online ASTER GDEM serves as a reasonably good alternative as a source of study for DEM data.

## ACKNOWLEDGEMENTS

The researchers would like to thank the Ministry of Higher Education (MOHE) of Malaysia for the FRGS Grant. We also, thank the Malaysian Centre for Geospatial Data Infrastructure (MaCGDI) for providing all the required Geodata. Besides, we would like to thank Ms. Hemalatha Kalimuthu for pre-processing the DEM data.

## REFERENCES

Arun, P., 2013. A comparative analysis of different DEM interpolation methods. Egypt. J. Remote Sens. Space Sci., 16: 133-139.

Beucher, S., 1994. Interpolation of sets, partitions and functions. Ecole des Mines of Paris, Paris, France. (In French)

Costa-Cabral, M.C. and S.J. Burges, 1994. Digital elevation model networks (DEMON): A model of flow over hillslopes for computation of contributing and dispersal areas. Water Resour. Res., 30: 1681-1692.

Erdogan, S., 2009. A comparision of interpolation methods. Earth Surf. Process. Landforms, 34: 366-376.

Iwanowski, M. and J. Serra, 2000. The Morphological-Affine Object Deformation. In: Mathematical Morphology and its Applications to Image and Signal Processing, Goutsias, J., L. Vincent and D.S.B. Berg (Eds.). Kluwer Academic Publishers, New York, USA., pp: 81-90.

Iwanowski, M., 2000. Application of mathematical morphology to image interpolation. Ph.D Thesis, Warsaw University of Technology, Warsaw, Poland.

Iwanowski, M., 2002. Image morphing based on morphological interpolation combined with linear filtering. Intl. J. WSCG., 1: 233-240.

Meyer, F., 1994. Interpolations. Ecole des Mines de Paris, Paris, France.

Meyer, F., 1996. A Morphological Interpolation Method for Mosaic Images. In: Mathematical Morphology and its Applications to Image and Signal Processing, Maragos, F.P., R. Schafer and M. Butt (Eds.). Springer, New York, USA., ISBN:978-1-4613-8063-4, pp: 337-344.

Serra, J., 1983. Image Analysis Mathematical Morphology. Academic Press, London, UK., ISBN: 10: 0126372403, pp: 610.

Serra, J., 1998. Hausdorff Distances and Interpolations. In: Mathematical Morphology and its Applications to Images and Signal Processing, Heijmans, H.J.A.M. and J. Roerdink (Eds.). Kluwer Academics Publishers, Dordrecht, Netherlands, ISBN:0-7923-5133-9, pp: 107-114.

Shingare, P. and M.S.S. Kale, 2013. Review on digital elevation model. Intl. J. Mod. Eng. Res., 3: 2412-2418.

Soille, P., 1994. Generalized Geodesic Distances Applied to Interpolation and Shape Description. In: Mathematical Morphology and its Applications to Image and Signal Processing, Serra, J. and P. Soille (Eds.). Springer, Netherlands, ISBN:978-94-010-4453-0, pp: 193-200.

Wolock, M.D. and C.V. Price, 1994. Effects of digital elevation model map scale and data resolution on a topography-based watershed model. Water Resour. Res., 30: 3041-3052.

Zhang, W. and D.R. Montgomery, 1994. Digital elevation model grid size, landscape representation and hydrologic simulations. Water Resour. Res., 30: 1019-1028.